A ^{31}P NMR Study of Solid Compounds $M_xP_2O_7$

Stephan Dusold, Jörg Kümmerlen, and Angelika Sebald*

Bayerisches Geoinstitut, Universität Bayreuth, D-95440 Bayreuth, Germany

Received: April 1, 1997; In Final Form: June 10, 1997[⊗]

The ^{31}P solid-state NMR properties of the pyrophosphate moiety for spatially well isolated $P_2O_7^{4-}$ units (such as in $Na_4P_2O_7{\cdot}10H_2O$) and for spatially nonisolated $P_2O_7^{4-}$ units (such as in $Cd_2P_2O_7$) are compared to each other. The properties of these two types of ^{31}P spin systems under conditions of magic angle spinning (MAS), of two-dimensional spin−echo experiments and rf-driven spin-diffusion experiments on nonspinning samples are investigated. The magnitude of $^2J(^{31}P_A{}^{31}P_B)$ is determined experimentally for $Cd_2P_2O_7$.

Introduction

The pyrophosphate anion $P_2O_7^{4-}$ represents an important moiety in numerous solid inorganic phosphate systems, both crystalline and amorphous. In terms of ^{31}P solid-state NMR, the $P_2O_7^{4-}$ unit itself is typically characterized by the simultaneous presence of considerable ^{31}P chemical shielding anisotropies (csa) and of homonuclear direct (*D*) and indirect (*J*) coupling (Scheme 1).

Relative magnitudes and orientations of anisotropic internal ^{31}P NMR interactions for the pyrophosphate unit are such that almost always the Hamiltonian of the corresponding ^{31}P spin system will be homogeneous in the sense of Maricq and Waugh[1] with, for instance, concomitant B_0 and MAS frequency-dependent higher order effects occurring in the respective ^{31}P MAS NMR spectra.[2−6] Whether or not the two ^{31}P spins within a $P_2O_7^{4-}$ unit of a given solid pyrophosphate may be described as an isolated, coupled homonuclear spin pair, depends on the degree of mutual spatial isolation of individual $P_2O_7^{4-}$ units in the respective three-dimensional solid-state structure. The question of isolated versus nonisolated ^{31}P spin pair NMR circumstances also depends on the choice of NMR experiment performed, that is, on the effective Hamiltonian appropriate to describe the ^{31}P spin system when subjected to a particular manipulation.

We have chosen two different types of crystalline pyrophosphates in order to further investigate and compare the properties of their ^{31}P spin systems under conditions of straightforward 1D ^{31}P MAS, of ^{31}P spin echo[7] and rf-driven spin diffusion[8,9] experiments on nonspinning samples and of purely homonuclear *J*-coupling-mediated polarization transfer.[10] Owing to the presence of H_2O in the crystalline lattice, $Na_4P_2O_7{\cdot}10H_2O$, **1**, contains a $P_2O_7^{4-}$ ^{31}P spin system which, to a very high degree of accuracy, may be described as an isolated homonuclear spin pair. In fact, **1** has previously been used as a model case of an isolated homonuclear ^{31}P spin pair for the simulation of the full spectral line shape of coupled isolated homonuclear spin pairs under MAS[3] and also for the illustration of the performance of a 2D spin−echo experiment for the extraction of orientational parameters for an isolated homonuclear spin pair.[7] We shall continue to use **1** as the isolated $P_2O_7^{4-}$ ^{31}P spin pair model case, and we will compare this spin system to the ^{31}P spin system in solid $Cd_2P_2O_7$, **2**, for which a much lesser degree of mutual spatial isolation of the individual $P_2O_7^{4-}$ units prevails.

Experimental Section

$Na_4P_2O_7{\cdot}10H_2O$, **1**, is commercially available (Aldrich Chemicals) and has been used without further purification. $Cd_2P_2O_7$, **2**, has been synthesized following a published procedure;[11] the identity and purity of our sample of **2** have been carefully checked by powder X-ray diffraction methods.

SCHEME 1: P−O−P Fragment in a Typical $P_2O_7^{4-}$ Unit[a]

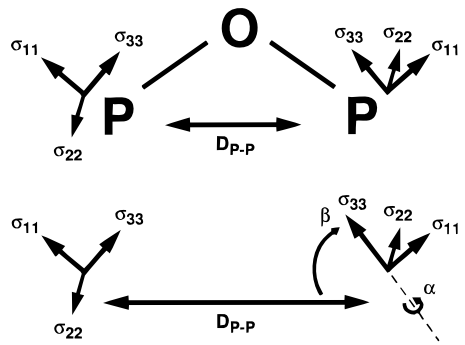

[a] Illustrated are the axes and directions of rotations for the Euler angles α and β to describe the orientation of the ^{31}P chemical shielding tensors relative to the intra-$P_2O_7^{4-}$ dipolar axis.

All ^{31}P NMR experiments were carried out at ^{31}P Larmor frequencies of 81.0 and 121.5 MHz, using Bruker MSL 200 and MSL 300 NMR spectrometers, respectively. Standard double-bearing probes and ZrO_2 rotors (4 and 7 mm diameter) were used, MAS frequencies ranged from 1800 to 9000 Hz and were actively controlled for stability within ±2 Hz (using a home-built device), and $\pi/2$ pulse durations were 2.0−3.5 μs. All NMR experiments on **1** employed ^{1}H−^{31}P Hartmann−Hahn cross-polarization (CP) and ^{1}H high-power decoupling. Recycle delays for CP experiments on **1** were 4 s, while direct single-pulse ^{31}P excitation on **2** required recycle delays of 20 s. Isotropic ^{31}P chemical shifts are quoted with respect to external 85% $H_3PO_4 \equiv 0$ ppm and Haeberlen's notation[12] is used to report eigenvalues of chemical shielding tensors. Phases and amplitudes of rf pulses were optimized using the ^{31}P resonance of a saturated $CHCl_3$ solution of *trans*-$(Et_3P)_2PdCl_2$. Phase cycling for all 2D experiments was according to the TPPI method.[13]

The pulse sequences of the TOBSY experiment[10] of the 2D spin−echo experiment[7] and of the rf-driven spin-diffusion experiment (WALTZ-17[14]) are shown in Scheme 2.

For one-dimensional ^{31}P TOBSY experiments (see Scheme 2a) as a function of mixing time τ_{mix} on **2** at $\nu_0 = 81.0$ and 121.5 MHz, stroboscopic sampling was employed, with the dwell time DW chosen such that the rotor period $T_{rot} = n$DW. τ_{inv} was adjusted to obtain an initial condition of complete inversion of one of the two resonances for $\tau_{mix} = 0$ ms. 128

[⊗] Abstract published in *Advance ACS Abstracts,* August 1, 1997.

S1089-5639(97)01142-0 CCC: $14.00

SCHEME 2: Pulse Sequences of (a) TOBSY Experiment,[10] (b) 2D Spin−Echo Experiment,[7] and (c) rf-Driven Spin-Diffusion Experiment[8,9,14]

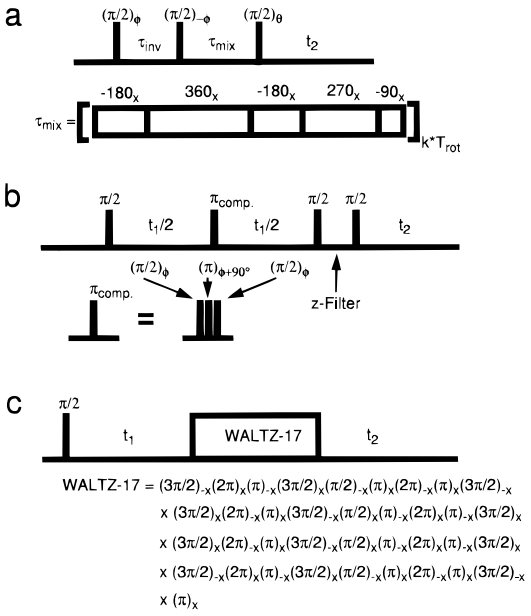

transients were accumulated for each mixing time. For all ^{31}P TOBSY experiments the condition $k = 8$ (see ref 10) was fulfilled: at $\nu_0 = 121.5$ MHz the $\pi/2$ pulse duration was 2.0 μs, and the spinning frequency was 5208 Hz, at $\nu_0 = 81.0$ MHz a $\pi/2$ pulse duration of 3.5 μs and a spinning frequency of 2976 Hz were used.

In the two-dimensional 81.0 MHz ^{31}P spin−echo experiments on nonspinning samples of **1** and **2** (see Scheme 2b) the plain π pulse was replaced by a composite π pulse[15] in the t_1 period. Typically 128 transients were accumulated per t_1 increment.

^{31}P spin-diffusion experiments under static conditions on **1** and **2** were carried out at $\nu_0 = 121.5$ MHz (see Scheme 2c). The WALTZ-17 pulse sequence[14] was applied during the mixing time τ_{mix}.

The programs for simulations of the 1D ^{31}P MAS NMR spectra are based on eq 17 in ref 3, those for simulation of the static spin−echo experiment are based on eqs 5 and 7 in ref 7. Calculations of 2D spin-diffusion powder patterns were according to eq 3 in ref 8a. Nonlinear least-mean-squares fits employed the MATLAB[16] simplex routine; the simulation programs utilized the GAMMA[17] programming package.

Results and Discussion

The single-crystal X-ray structures of $Na_4P_2O_7 \cdot 10H_2O$, **1**,[18] and $Cd_2P_2O_7$, **2**,[11] are known. The two P atoms within the $P_2O_7^{4-}$ unit of **1** are crystallographically equivalent with a C_2 symmetry axis, bisecting the P−O−P bond angle, relating the two sites. Hence, the two ^{31}P spins in the $P_2O_7^{4-}$ unit of **1** constitute an isolated spin pair with identical eigenvalues of the two csa tensors but differing orientation of these two tensors in the crystal axes system. This type of spin system may also be described as representing a case of $n = 0$ rotational resonance.[2−5] The P−O−P bond angle in **1** is 130° and the P−P distance within the $P_2O_7^{4-}$ unit is 292 pm,[18] corresponding to $D = 791$ Hz.

The two P atoms within the $P_2O_7^{4-}$ unit in **2** are crystallographically inequivalent, the P−O−P bond angle for **2** is 132°, and the P−P distance within this $P_2O_7^{4-}$ unit is 297 pm ($D =$ 752 Hz). The three-dimensional structure of solid **2** is such that within a radius of 440 pm each P atom is in addition surrounded by another nine P atoms.[11] This is a typical condition for solids of the type $M_xP_2O_7$ in the absence of further "spacers" in the structure (such as, for instance, the H_2O molecules in the structure of solid **1**). Disregarding these multiple inter-$P_2O_7^{4-}$ contacts to further ^{31}P spins, the ^{31}P spin system in solid **2** may be named an AB spin system, merely reflecting the crystallographic nonequivalence of the two ^{31}P spins within the $P_2O_7^{4-}$ unit. To what extent the lack of mutual spatial isolation for the ^{31}P spin system in **2** (in comparison with the isolated ^{31}P spin pair in **1**) is reflected in various solid-state NMR experiments is discussed in the following.

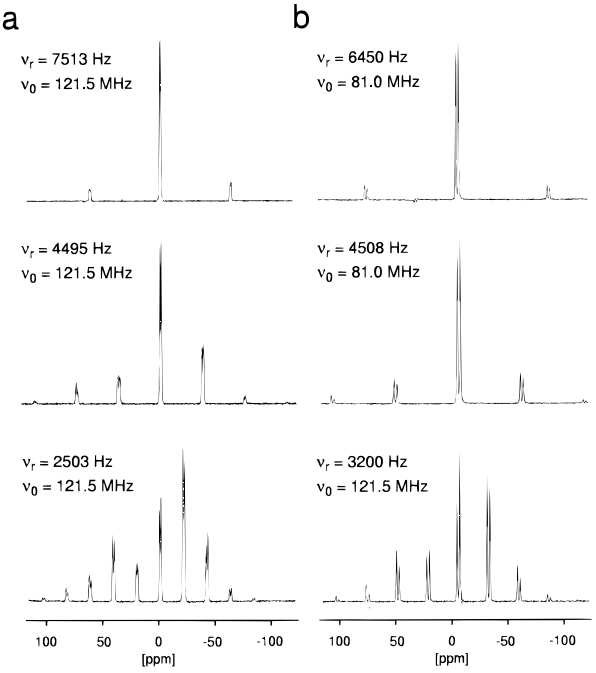

Figure 1. Experimental ^{31}P MAS NMR spectra of (a) $Na_4P_2O_7 \cdot 10H_2O$, **1**, and (b) $Cd_2P_2O_7$, **2**, obtained at $\nu_0 = 81.0$ MHz and $\nu_0 = 121.5$ MHz and at different MAS frequencies ν_r as indicated.

^{31}P MAS NMR of 1 and 2. ^{31}P MAS NMR spectra of **1** and **2** obtained at various different MAS frequencies are shown in Figure 1. For the AA′ ^{31}P spin pair in $Na_4P_2O_7 \cdot 10H_2O$, **1** (see Figure 1a), even for a MAS frequency of $\nu_{rot} = 7$ kHz (ν_0 = 121.5 MHz), corresponding to roughly 10 times the magnitude of the homonuclear dipolar coupling within the spin pair, the ^{31}P resonance of **1** still displays splitting. Kubo and McDowell have derived an approximation to calculate the full spectral line shape of MAS NMR spectra of isolated dipolar (and J) coupled homonuclear spin pairs and have simulated ^{31}P MAS NMR spectra of **1**.[3] Using eq 17 in their paper for the simulation of our ^{31}P MAS spectra of **1**, we find good agreement between experimental and calculated data for a fairly wide range of experimental conditions. A fitting of experimental ^{31}P MAS NMR spectra of **1**, obtained at two different external magnetic field strengths and at various different MAS frequencies, yields the ^{31}P NMR parameters for **1** given in Table 1; our values of the principal components of the ^{31}P shielding tensors for **1** are in agreement with the previously reported results.[3] From iterative fitting of ^{31}P MAS NMR spectra of **1** alone, however, we find an ambiguity concerning the angle β: it is not possible to distinguish the two cases with $\beta = 23°$ and $\beta = 40°$ (see Table 1). With β describing the deviation of the σ_{33} component of the shielding tensor from the direction of the dipolar axis, with σ_{33} being the least shielded tensor component and with a P−O−P bond angle of 130°,[18] $\beta = 23°$ would correspond to an orientation of the least shielded tensor component nearly coincident with the P−$O_{central}$ bond direction in the $P_2O_7^{4-}$ anion

TABLE 1: ^{31}P NMR Parameters for $Na_4P_2O_7 \cdot 10H_2O$, 1, and $Cd_2P_2O_7$, 2, As Determined from Fitting of ^{31}P MAS NMR Spectra[a]

	σ_{iso} [ppm]	σ_{11} [ppm]	σ_{22} [ppm]	σ_{33} [ppm]	η	α [deg]	β [deg]
1	+2.3	55 ± 4	30 ± 4	−78 ± 1	0.30 ± 0.1	−26 ± 1	−23 ± 2
	(+2.3	55 ± 4	30 ± 1	−79 ± 3	0.30 ± 0.1	−26 ± 1	−40 ± 2)[b]
2							
$^{31}P_A$	+3.1	58 ± 1	32 ± 3	−80 ± 2	0.31 ± 0.1	*c*	154 ± 5
$^{31}P_B$	+5.1	52 ± 4	26 ± 3	−63 ± 3	0.38 ± 0.1	*c*	−26 ± 5

[a] Euler angles α, β as defined in Scheme 1; γ is omitted because γ is arbitrary for **1** and could not be determined for **2**. Definitions of shielding parameters according to Haeberlen:[12] $\delta_{iso} = -\sigma_{iso}$; $|\sigma_{33} - \sigma_{iso}| \geq |\sigma_{11} - \sigma_{iso}| \geq |\sigma_{22} - \sigma_{iso}|$; asymmetry parameter $\eta = (\sigma_{22} - \sigma_{11})(\sigma_{33} - \sigma_{iso})^{-1}$. [b] Given in brackets: second set of parameters, obtained from fitting of ^{31}P MAS NMR spectra of **1**; indistinguishable from correct solution from ^{31}P MAS NMR alone, but excluded by 2D spin−echo experiment (see text). [c] α_A, α_B not given because not significantly defined from fitting of ^{31}P MAS NMR spectra of **2**.

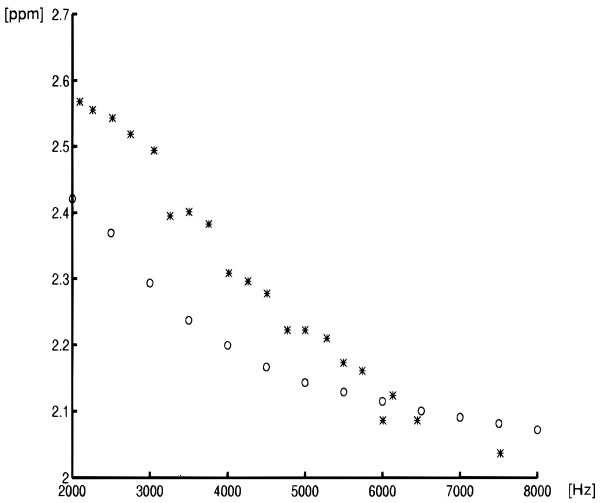

Figure 2. Splitting $\Delta\nu$ [ppm] between zeroth-order spinning sidebands of the two ^{31}P resonances of **2** as a function of MAS frequency ν_r [Hz] at ν_0 = 81.0 MHz (*). Also shown is the splitting $\Delta\nu$ [ppm] as determined from line-shape simulations of ^{31}P MAS NMR spectra of **2** (○); see Figure 3.

in solid **1**. How this remaining ambiguity in orientational parameters can be resolved will be shown below.

The 121.5 MHz ^{31}P MAS NMR spectra of $Cd_2P_2O_7$, **2** (see Figure 1b), clearly show the presence of two ^{31}P resonances with different isotropic (and anisotropic) chemical shifts, in accord with the presence of two crystallographically inequivalent P sites in the $P_2O_7^{4-}$ moiety in solid **2**.[11] In comparison with the massive MAS frequency-dependent line shape changes observed for the AA′ spin pair in **1**, the MAS frequency-dependent effects on the spectral line shape for the AB spin system in **2** at first glance seem negligible. That a difference in isotropic ^{31}P chemical shift for the AB spin system in **2** of ca. 2 ppm is not sufficient to completely quench all higher order effects in ^{31}P MAS NMR spectra of **2** is evident from Figure 2. A plot of $\Delta\nu$ (where $\Delta\nu$ [ppm] is the splitting between the zeroth-order spinning sidebands of the two ^{31}P resonances) vs MAS frequency clearly shows $\Delta\nu$ to be dependent on MAS frequency. Similar effects have been described previously for ^{31}P MAS NMR spectra of several other solid pyrophosphates.[19] Dependence of $\Delta\nu$ on the respective MAS frequency disqualifies a single-spin approximation as an appropriate way to extract ^{31}P chemical shielding tensor eigenvalues from ^{31}P MAS NMR spectra of **2**. For the regime of relatively high MAS frequencies an approximation for $\Delta\nu$, allowing to calculate the isotropic chemical shift difference $\Delta\nu_{iso}$ for an isolated AB spin pair, has been given:[20]

$$\Delta\nu = \sqrt{(\Delta\nu_{iso})^2 + J^2 + K^2}$$

where $K = C(\alpha,\beta,\gamma)/\nu_{rot}$ is the second-order perturbation term

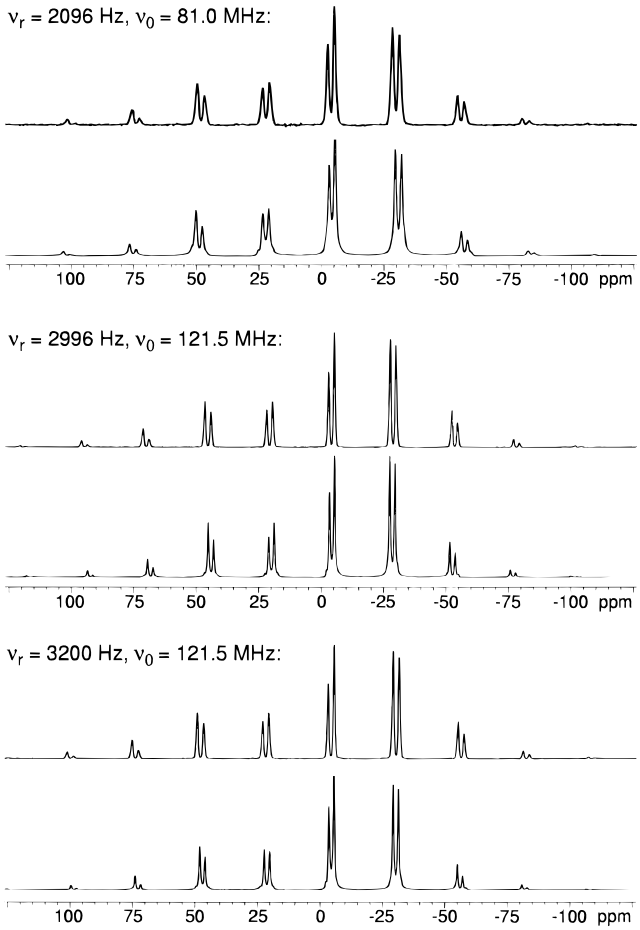

Figure 3. Comparison of experimental (top trace) and simulated (bottom trace) ^{31}P MAS NMR spectra of $Cd_2P_2O_7$, **2**. Larmor frequencies ν_0 and MAS frequencies ν_r as indicated.

as defined by Maricq and Waugh[1] and with *C* being a constant depending on the crystallite orientation in the rotor axis system. An isotropic chemical shift difference $\Delta\nu_{iso} = 1.95 \pm 0.05$ ppm for the two ^{31}P resonances in **2** is determined from the experimental $\Delta\nu$ values shown in Figure 2. The magnitude of $^2J(^{31}P_A{}^{31}P_B) = 23 \pm 4$ Hz for solid **2** has been determined independently (see below), and the magnitude of $D = 752$ Hz can be calculated from the known P_A-P_B internuclear distance. $\Delta\nu_{iso}$ and the magnitudes of *J* and *D* serve as known input parameters for simulations of ^{31}P MAS spectra of **2**, using again the two-spin approximation as described by Kubo and McDowell.[3] A comparison of experimental and simulated ^{31}P MAS NMR spectra of **2** is shown in Figure 3. The experimentally obtained ^{31}P MAS NMR spectra of **2** are well reproduced, including the magnitude of $\Delta\nu$ as a function of spinning frequency (see Figure 2, where $\Delta\nu$ determined from line shape simulations is shown in comparison to the experimentally

determined data). Fitting of several ^{31}P MAS NMR spectra, obtained at different MAS frequencies and different external magnetic field strengths, yields the csa eigenvalues and orientation parameters for $^{31}P_A$ and $^{31}P_B$ given in Table 1. With a P−O−P bond angle of 132°, Euler angles $\beta_A = 154°$ and $\beta_B = 26°$ would describe an orientation of both ^{31}P chemical shielding tensors in **2** with the least shielded component collinear with the respective $P-O_{central}$ bond direction. It should be noted, however, that spectral line-shape simulations of ^{31}P MAS NMR spectra of **2** are far more sensitive to changes in magnitude of the chemical shielding tensor components than to changes in orientational parameters. The minima found for the Euler angles β_A, β_B are considerably shallower than, e.g., the minima for β found for **1**. The orientational parameters derived from line-shape simulations of ^{31}P MAS NMR spectra of **2** thus require further independent confirmation (see below). We find significant differences in ^{31}P chemical shielding anisotropy and asymmetry parameters for the two crystallographically inequivalent P sites in the $P_2O_7^{4-}$ unit of **2** but unambiguous assignment of the two $^{31}P_A$, $^{31}P_B$ resonances to the two crystallographic P sites, based on these data, is not possible.

One-Dimensional ^{31}P TOBSY of 2. The magnitude of $^2J(^{31}P_A{}^{31}P_B)$ in typical $P_2O_7^{4-}$ moieties has so far not been determined experimentally; for spectral line-shape simulations of ^{31}P MAS NMR spectra of **1**,[3] J has been assumed to be negligible. Baldus and Meier have recently introduced a pulse sequence (TOBSY),[10] where both dipolar interactions and chemical shifts are suppressed during a rotor-synchronized mixing time τ_{mix} (see Scheme 2a). Under these conditions, polarization transfer during τ_{mix} is mediated by homonuclear J coupling only. The magnitude of J for a homonuclear AB spin pair can thus be determined from the oscillatory dependence of the transfer on the mixing time; resolved J coupling in the corresponding 1D MAS NMR spectra is not a necessary prerequisite. The results of a one-dimensional ^{31}P TOBSY experiment on **2** are shown in Figure 4. The initial condition of complete inversion of one of the two ^{31}P resonances for $\tau_{mix} = 0$ ms is illustrated in Figure 4a; the dependence of the amplitude of the noninverted resonance on τ_{mix} is shown in Figure 4b.

Within experimental error, the one-dimensional ^{31}P TOBSY experiment on **2** at $\nu_0 = 81.0$ and 121.5 MHz yields identical values for $^2J(^{31}P_A{}^{31}P_B) = 23 \pm 4$ Hz, proving that for $k = 8$[10] indeed there are no residual contributions from incompletely suppressed csa terms to the oscillatory transfer observed as a function of mixing time. With the magnitude of J, the one-dimensional version of the TOBSY experiment provides information about an important input parameter for simulations of MAS spectra of isolated homonuclear AB spin pairs in general. The determination of the magnitude of $^2J(^{31}P_A{}^{31}P_B)$ for **2** a posteriori also justifies the assumption made (negligible contribution from J)[3] for spectral line-shape simulations of ^{31}P MAS NMR spectra of **1**: variation of J within 0 ± 25 Hz does not significantly alter the results of line-shape simulations of ^{31}P MAS NMR spectra of **1** and **2**.

Two-Dimensional ^{31}P Spin−Echo Experiments on 1 and 2. As mentioned above, fitting of ^{31}P MAS NMR spectra of **1** alone leaves an ambiguity with respect to the Euler angle β. The 2D spin−echo experiment (see Scheme 2b) on static powder samples has been shown[7] to yield accurate orientational parameters for isolated coupled homonuclear spin pairs; in fact, the experiment has been demonstrated on **1**. The 2D spin−echo experiment is well suited as a complement to iterative fitting of ^{31}P MAS NMR spectra of isolated spin pairs.[21] With respect to the remaining ambiguity from fitting of ^{31}P MAS NMR spectra of **1**, the 2D spin−echo experiment on **1** resolves this problem. This is illustrated in Figure 5, where the contour plot of the experimental spectrum (Figure 5a) is shown in comparison to simulated contour plots for $\beta = 23°$ (Figure 5b) and $\beta = 40°$ (Figure 5c). Also shown is a plot of the deviation between experimental and simulated data where β is varied between 0 and 180° (Figure 5d). Fitting of the 2D ^{31}P spin−

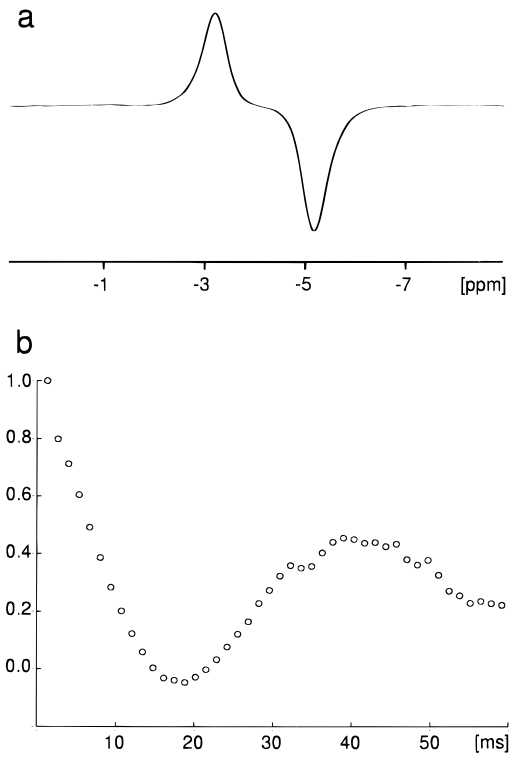

Figure 4. ^{31}P TOBSY experiment[10] on $Cd_2P_2O_7$, **2**: (a) initial condition for $\tau_{mix} = 0$ ms; (b) experimentally determined amplitudes of the noninverted resonance as a function of τ_{mix} [ms] at $\nu_0 = 81.0$ MHz; the vertical axis is scaled such that the relative amplitude of this resonance is 1 for $\tau_{mix} = 0$ ms.

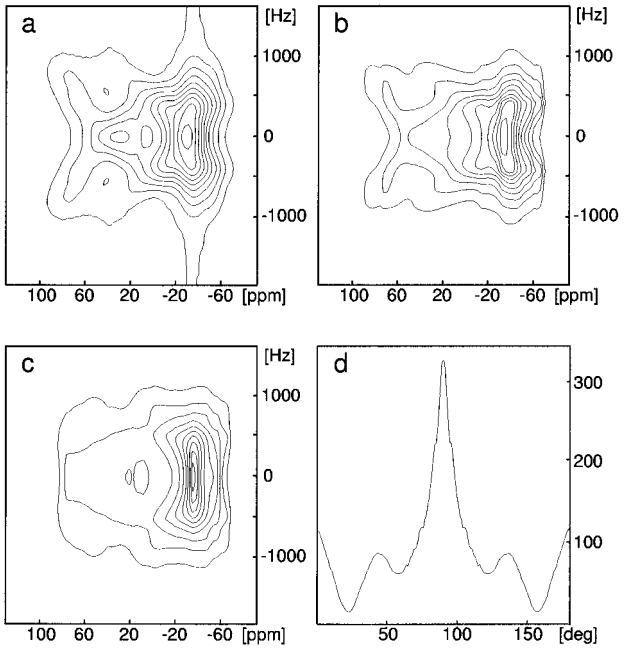

Figure 5. 2D ^{31}P spin−echo experiment on $Na_4P_2O_7 \cdot 10H_2O$, **1**. (a) Contour plot of experimental spectrum, obtained at $\nu_0 = 81.0$ MHz. (b) Simulated contour plot for $\beta = 23°$; (c) simulated contour plot for $\beta = 40°$. (d) Plot of deviation [au] between calculated and experimental data as a function of β.

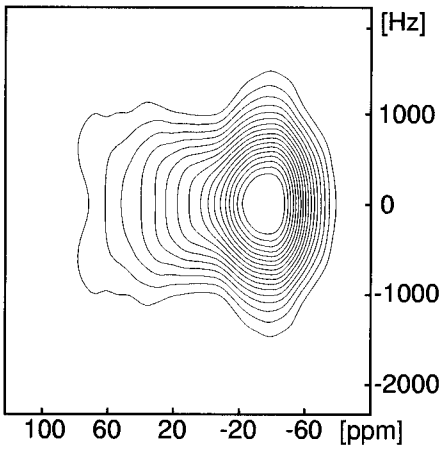

Figure 6. Contour plot of the experimental ^{31}P 2D spin−echo spectrum (ν_0 = 81.0 MHz) of **2**.

echo spectrum of **1** clearly selects $\beta = 23°$ as the correct solution, for which the orientation of the least-shielded component of the ^{31}P chemical shielding tensors in **1** nearly coincides with the direction of the P−$O_{central}$ bond direction in the $P_2O_7^{4-}$ unit.

Spectral line-shape simulations of ^{31}P MAS NMR spectra of **2**, obtained within a two-spin approximation, also yield parameters for the two inequivalent ^{31}P spins A, B in the $P_2O_7^{4-}$ unit of **2** corresponding to an orientation of the least-shielded tensor components along the respective P−$O_{central}$ bond direction (see Table 1). As pointed out above, it would be highly desirable to obtain independent confirmation of these results, owing to the limited sensitivity of the ^{31}P MAS NMR line shapes for **2** to orientational parameters. Figure 6 depicts the contour plot of the experimental ^{31}P 2D spin−echo spectrum of **2**, obtained under identical conditions as the 2D spin−echo spectrum of **1** (see Figure 5a). Other than for the isolated ^{31}P spin pair in **1**, the spin−echo spectrum of **2** lacks all fine structure, no orientational information may be derived from this experiment. In contrast, the ^{31}P 2D spin−echo experiment under static conditions on **2** quite impressively illustrates the nonisolated character of the $^{31}P_A$−$^{31}P_B$ spin pair in the $P_2O_7^{4-}$ moiety of **2**.

RF-Driven ^{31}P Spin-Diffusion Experiments on 1 and 2. Two-dimensional spin-diffusion experiments on static powder samples can yield accurate information on relative chemical shielding tensor orientations.[8,9] Under suitable experimental conditions, that is for mixing times long enough to ensure complete exchange, the resulting powder patterns may be analyzed with respect to the Euler angles describing the relative orientations of the two ^{31}P chemical shielding tensors within the $P_2O_7^{4-}$ unit. When driving the ^{31}P spin diffusion by applying the WALTZ-17 sequence[9,14] during the mixing time, a condition of quasi-equilibrium for **1** and **2** is reached for τ_{mix} = 100 ms. Contour plots of the resulting 2D powder patterns for **1** and **2** are shown in Figure 7 a,b. The patterns of the experimental spectra for **1** and **2** are very similar because of the presence of not more than one differently oriented $P_2O_7^{4-}$ unit in the asymmetric unit of **1** and **2**. Also shown (Figure 7c,d) are simulated contour plots, based on the ^{31}P NMR parameters for **1** (see Table 1): the simulation corresponding to $\beta = 25°$ (i.e., taking the least-shielded components of the two ^{31}P shielding tensors as collinear with the P−$O_{central}$ bond directions, with an angle $\vartheta = 130°$ between them) is in agreement with the experimental results on **1** and **2**. Variation of the angle ϑ in simulations leads to disagreement, as is illustrated in Figure 7d for $\vartheta = 180°$. Qualitative inspection of the simulated contour plot in Figure 7c confirms the

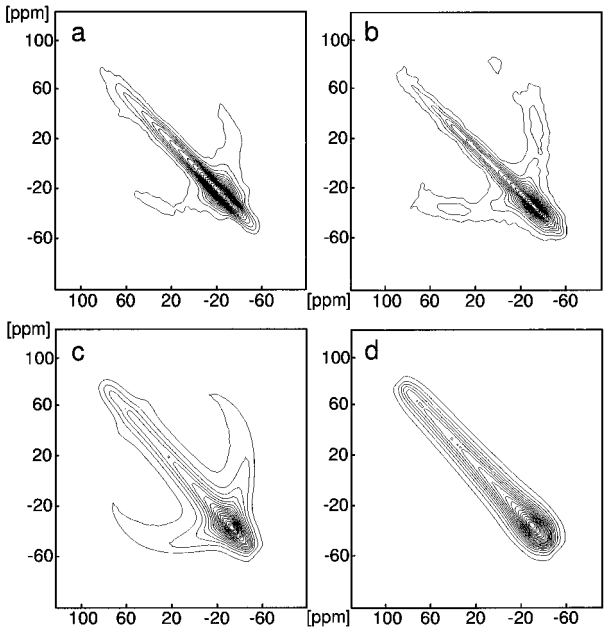

Figure 7. Contour plots of 2D ^{31}P spin-diffusion spectra. (a) Experimental spectrum (ν_0 = 121.5 MHz) of **2**; (b) experimental spectrum (ν_0 = 121.5 MHz) of **1**; (c) contour plot, calculated for the ^{31}P NMR parameters of **1** (see Table 1), with the angle $\vartheta = 130°$ describing the mutual relative directions of the least-shielded components of the two ^{31}P chemical shielding tensors in the $P_2O_7^{4-}$ unit; (d) same as (c) but $\vartheta = 180°$.

orientational parameters for the ^{31}P shielding tensors in **1** and **2** as derived from fitting of the ^{31}P MAS NMR spectra of **1** and **2**.

To briefly summarize the results: Owing to the through-bond transfer mechanism, the TOBSY experiment on **2** selectively monitors an intra-$P_2O_7^{4-}$ connectivity also under conditions of spatially nonisolated ^{31}P spins. At the other extreme, the 2D spin−echo experiment on **2** emphasizes the lack of mutual spatial isolation of the $P_2O_7^{4-}$ units in solid **2**. One-dimensional ^{31}P MAS NMR spectra of **2** appear as largely dominated by intra-$P_2O_7^{4-}$ mutual ^{31}P−^{31}P interactions, and rf-driven spin-diffusion experiments on **2** under static conditions confirm the parameters obtained from line-shape simulations of ^{31}P MAS NMR spectra.

Conclusions

The ^{31}P spin system in solid pyrophosphates, regardless of whether we have to deal with the isolated ^{31}P spin-pair variety (such as in **1**) or with the nonisolated $P_2O_7^{4-}$ ^{31}P spin-pair variety (such as in **2**), usually cannot be adequately described within a single-spin approximation. While the failure of single-spin approximations for both types of $P_2O_7^{4-}$ ^{31}P spin systems and the validity of a two-spin approximation for isolated ^{31}P spin pairs, such as in **1**, are easily demonstrated, use of a two-spin approximation for the description of pyrophosphate ^{31}P spin systems such as in **2** can be considered only a next-best approximation. There is little room to soundly evaluate the remaining errors involved when operating within a two-spin approximation for cases such as **2**, even if, for instance, within this approximation experimental ^{31}P MAS NMR data for a wide range of experimental conditions are well reproduced. With respect to the NMR properties of homonuclear ^{31}P spin systems in solid inorganic phosphates in general, pyrophosphates are to be considered a special case: pyrophosphates are the only type of condensed phosphate where there exists, in addition to the presence of large ^{31}P chemical shielding anisotropies, one dipolar

interaction (intra-$P_2O_7^{4-}$), the magnitude of which considerably exceeds the magnitude of the remaining, inter-$P_2O_7^{4-}$ homonuclear dipolar interactions. This particular pyrophosphate property may serve as some justification for the exploration of the applicability of a two-spin approximation for the description of the ^{31}P spin system in solid pyrophosphates such as **2**. No such distinctions in terms of one, more or less, dominating dipolar interaction in the spin system are, however, usually justified for other types of solid inorganic phosphates. The more important it seems that in general ^{31}P NMR investigations of connectivity patterns in solid phosphates, in addition and complementary to ^{31}P NMR experiments probing distance connectivities by homonuclear dipolar recoupling methods, should also employ ^{31}P NMR experiments probing through-bond connectivities by polarization transfer via homonuclear *J* coupling.[22]

Acknowledgment. Research funding by the Deutsche Forschungsgemeinschaft and the Fonds der Chemischen Industrie is gratefully acknowledged. We thank W. A. Dollase, University of California, Los Angeles, for his generous donation of the $Cd_2P_2O_7$ sample used in this study. We would further like to thank M. Baldus, R. Iuliucci, and B. H. Meier, University of Nijmegen, The Netherlands, for scientific discussions and for making information about the TOBSY experiment available to us prior to publication.

References and Notes

(1) Maricq, M. M.; Waugh, J. S. *J. Chem. Phys*. **1979**, *70*, 3300.

(2) Levitt, M. H.; Raleigh, D. P.; Creuzet, F.; Griffin, R. G. *J. Chem. Phys*. **1990**, *92*, 6347.

(3) Kubo, A.; McDowell, C. A. *J. Chem. Phys*. **1990**, *92*, 7156.

(4) Schmidt, A.; Vega, S. *J. Chem. Phys*. **1992**, *96*, 2655.

(5) Nielsen, N. C.; Creuzet, F.; Griffin, R. G.; Levitt, M. H. *J. Chem. Phys*. **1992**, *96*, 5668.

(6) Nakai, T.; McDowell, C. A. *Mol. Phys.* **1992**, *77*, 569.

(7) Nakai, T.; McDowell, C. A. *J. Am. Chem. Soc*. **1994**, *116*, 6373.

(8) (a) Robyr, P.; Meier, B. H.; Ernst, R. R. *Chem. Phys. Lett*. **1991**, *187*, 471. (b) Tycko, R; Dabbagh, G. *J. Am. Chem. Soc*. **1991**, *113*, 3592.

(9) Robyr, R.; Tomaselli, M.; Straka, J.; Grob-Pisano, C.; Suter, U. W.; Meier, B. H.; Ernst, R. R. *Mol. Phys*. **1995**, *84*, 995.

(10) Baldus, M.; Meier, B. H. *J. Magn. Reson. A* **1996**, *121*, 65.

(11) Calvo, C.; Au, P. K. *Can. J. Chem*. **1969**, *47*, 3409.

(12) Haeberlen, U. *High-Resolution NMR in Solids. Selective Averaging*; In: *Adv. Magn. Reson., Suppl. 1*; Academic Press: New York, 1976.

(13) Marion, D.; Wüthrich, K. *Biochem. Biophys. Res. Commun*. **1983**, *113*, 467.

(14) Shaka, A. J.; Keeler, J.; Freeman, R. *J. Magn. Reson*. **1983**, *53*, 313.

(15) Levitt, M. H. *Prog. Nucl. Magn. Reson. Spectrosc*. **1986**, *18*, 61.

(16) MATLAB, Version 4.2, The MathWorks Inc.: Natick, MA, 1994.

(17) Smith, S.; Levante, T.; Meier, B. H.; Ernst, R. R. *J. Magn. Reson. A* **1994**, *106*, 75.

(18) McDonald, W. S.; Cruickshank, D. W. *Acta Crystallogr*. **1967**, *22*, 43.

(19) a) Hayashi, S.; Hayamizu. K. *Chem. Phys. Lett*. **1989**, *161*, 158. (b) Hayashi, S.; Hayamizu, K. *Chem. Phys*. **1991**, *157*, 381.

(20) Challoner, R.; Nakai, T.; McDowell, C. A. *J. Magn. Reson*. **1991**, *94*, 433.

(21) Dusold, S.; Klaus, E.; Sebald, A.; Bak, M.; Nielsen, N. C. *J. Am. Chem. Soc*., in press.

(22) Baldus, M.; Iuliucci, R. J.; Meier, B. H. *J. Am. Chem. Soc*. **1997**, *119*, 1121.